

Volume production of D[−] negative ions in low-pressure D₂ plasmas—negative ion densities versus plasma parameters

Osamu Fukumasa and Shigefumi Mori

Department of Electrical and Electronic Engineering, Faculty of Engineering, Yamaguchi University, Tokiwadai 2-16-1, Ube 755-8611, Japan

Received 4 July 2005, accepted for publication 21 April 2006

Published 22 May 2006

Online at stacks.iop.org/NF/46/S287

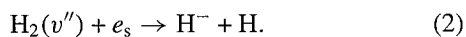
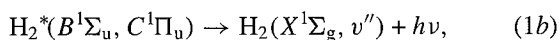
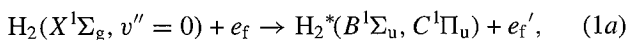
Abstract

Pure volume production of D[−] negative ions is studied in a rectangular arc chamber. Production and control of D₂ plasmas are tested by varying the intensity of the magnetic filter MF. The values of electron temperature T_e and electron density n_e in D₂ plasmas are slightly higher than those in H₂ plasmas. T_e in D₂ plasmas cannot be decreased below 1 eV in the extraction region with the same MF conditions for optimizing H₂ plasmas. A stronger MF field is required for controlling T_e in D₂ plasmas. Therefore, the transport in or the production of H₂ and D₂ plasmas is different, i.e. there is an isotope effect, a consequence of which is that the H[−] and D[−] densities have different spatial distributions. Extracted H[−] and D[−] currents are primarily determined by H[−] and D[−] densities in front of the extraction hole, respectively. According to the estimated rate coefficients and collision frequencies of main collision processes, it is reconfirmed that T_e in the extraction region should be maintained below 1 eV with n_e kept high for the enhancement of H[−] and D[−] production. For the enhancement of D[−] production, preliminary results on VUV emission measurement are presented and discussed briefly.

PACS numbers: 29.25.Ni, 52.20.−j, 52.20.Jm

1. Introduction

Sources of H[−] and D[−] negative ions are required for efficient generation of neutral beams with energies above ≈100 keV/nucleon. The magnetically filtered multicusp ion source has been shown to be a promising source of high-quality multiampere H[−] ions. In pure hydrogen (H₂) discharge plasmas, most of the H[−] ions are generated by dissociative attachment of slow plasma electrons e_s (electron temperature $T_e \sim 1$ eV) to highly vibrationally excited hydrogen molecules H₂(v'') (effective vibrational level $v'' \geq 5-6$). These H₂(v'') are mainly produced by collisional excitation of fast electrons e_f with energies in excess of 15–20 eV. Namely, H[−] ions are produced by the following two-step process [1, 2]:



where H₂($X^1\Sigma_g$) means the ground electronic state of the hydrogen molecule and H₂^{*}($B^1\Sigma_u$) and H₂^{*}($C^1\Pi_u$) mean the excited electronic states. The transitions from the $B^1\Sigma_u$ and $C^1\Pi_u$ levels to the ground state, $X^1\Sigma_g$, of H₂ are termed the

Lyman and Werner Bands, respectively, and are found in the vacuum ultraviolet (VUV) region.

The reaction-producing D[−] ions is believed to be the same as that for the production of H[−]. To develop efficient D[−] ion sources with high current density, it is important to clarify production and control of deuterium (D₂) plasmas and to understand the differences in the two-step process of negative ion production between H₂ plasmas and D₂ plasmas. Caesium (Cs) seeding of this type of ion source is often used as it enhances the extracted negative ion currents and reduces the extracted electron currents. There are some studies on optimization of volume-produced D[−] ions with or without Cs [3–5]. However, here we focus on understanding the negative ion production mechanisms in the ‘volume’ ion source where negative ions are produced in low-pressure pure H₂ or D₂ discharge plasmas.

For this purpose, we are interested in estimating densities of highly vibrationally excited molecules and negative ions in the source. The production process of H₂(v'') or D₂(v'') is discussed [6] by observing the photon emission, i.e. VUV emission associated with the process (1b) [7, 8]. To clarify the relationship between plasma parameters and volume production of negative ions, the densities of H[−] or D[−] ions in

the source are measured [9, 10] by the laser photodetachment method [11].

The influence of plasma parameter distributions on H^- or D^- production is discussed using estimated rate coefficients and collision frequencies based on measured plasma parameters [12–14]. Estimating negative ion densities in the source with the use of the laser photodetachment technique, we discuss the relationship between the negative ions in the source and the extracted negative ion currents [12]. For studying enhancement of D^- production, preliminary results on VUV emission measurements are also presented.

2. Experimental set-up

Figure 1(a) shows a schematic diagram of the ion source [9, 10, 12–14]. The rectangular arc chamber is 25 cm \times 25 cm in cross section and 19 cm in height. Four tungsten filaments 0.7 mm in diameter and 20 cm in length are installed in the source region from the side walls of the chamber. The line cusp magnetic field is produced by permanent magnets which surround the chamber. The external magnetic filter (MF) is composed of a pair of permanent magnets in front of the plasma grid (PG). Figure 1(b) shows profiles of the field intensities for five different MFs along the axis of the ion source. The different MFs are created by changing the distance between the pair of the permanent magnets. These MFs gradually separate the extraction region from the source region with filaments. In the present experiment, using these MFs, production and control of H_2 and D_2 plasmas to enhance negative ion volume production are studied. The end flange is kept at floating potential and the PG potential is kept at ground potential throughout the present experiments for both H_2 and D_2 plasmas.

In the source region, the VUV emission measurements related to the $H_2(v'')$ or $D_2(v'')$ production, i.e. the process (1b), are carried out using the VUV spectrometer. The spectrometer was normally operated at a wavelength resolution of 0.1 nm. The optical pipe is equipped with collimators such that a rectangular plasma volume with a cross section of about $6 \times 3 \text{ mm}^2$ is imaged. Emission intensity yields results averaged over the line of sight.

The plasma parameters are measured by an axially movable cylindrical Langmuir probe, supported by a quartz glass pipe with diameter of 3 mm. This probe is also used to measure negative ion density. Negative currents are extracted through a single hole 10 mm in diameter on the PG. These currents are introduced into a magnetic deflection type ion analyzer for relative measurements of the extracted H^- or D^- current. On the other hand, H^- or D^- densities in the source are measured by the laser photodetachment method [3, 11]. In this technique, the electron is detached from the negative ion by means of a pulsed laser beam and collected by the cylindrical tungsten probe (1 mm in diameter, 6 mm long) placed along the axis of the laser beam. The probe is biased at +10 V relative to the anode and therefore it attracts the detached electrons. This creates a probe current pulse, Δi^- , whose height is proportional to the negative ion density. The dc current to the probe, i_{dc} , is proportional to n_e . Then the measured ratio $\Delta i^- / i_{dc}$ gives the relative negative ion density n_- / n_e . A light pulse from a Nd:YAG laser (100 mJ cm $^{-2}$ pulse, wavelength 1064 nm, duration of laser pulse 9 ns, repetition 10 Hz) is

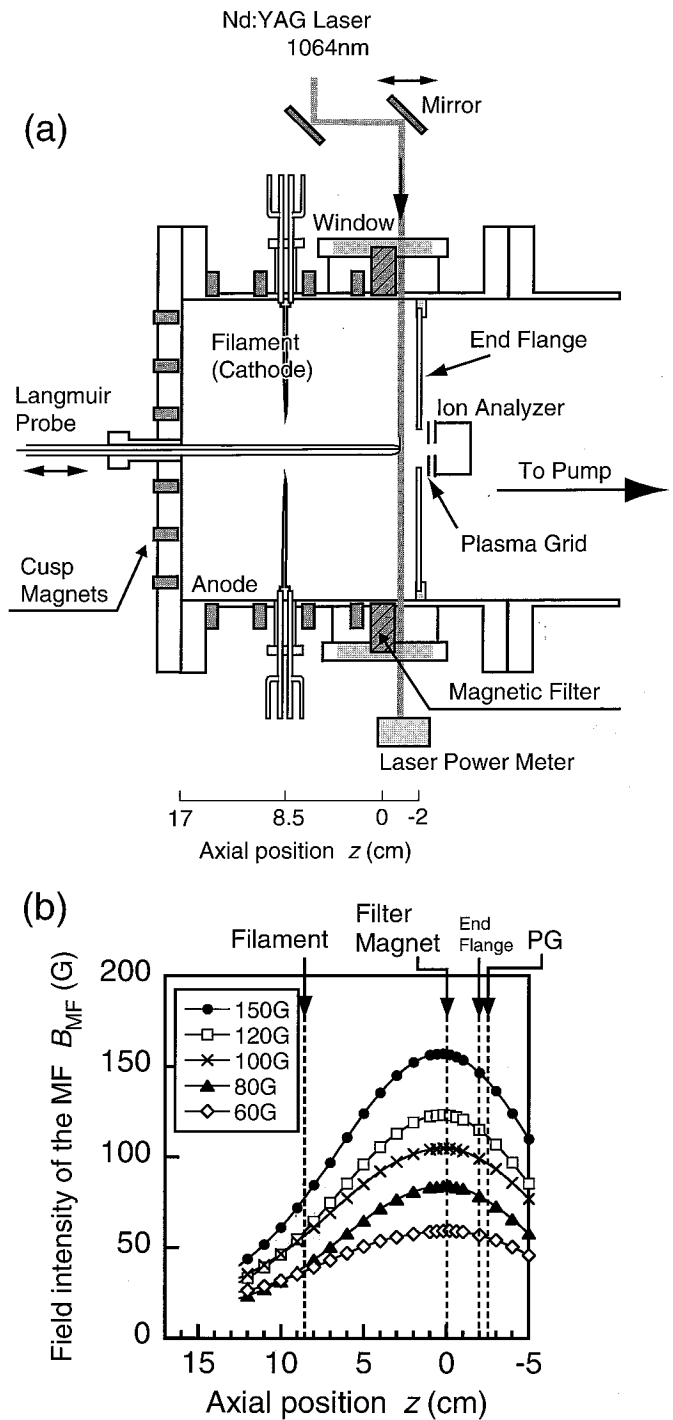


Figure 1. (a) Schematic diagram of the ion source. The probe, the laser path and power meter used in photo-detachment experiments are also shown. (b) Axial distributions of field intensities for the five different MFs.

introduced from the side wall window of the chamber and passes through the source plasmas. The laser light axis can move across the MF.

3. Experimental results and discussion

3.1. Production and control of D_2 plasmas

On H^-/D^- volume production, the desired condition for plasma parameters is as follows: T_e in the extraction region

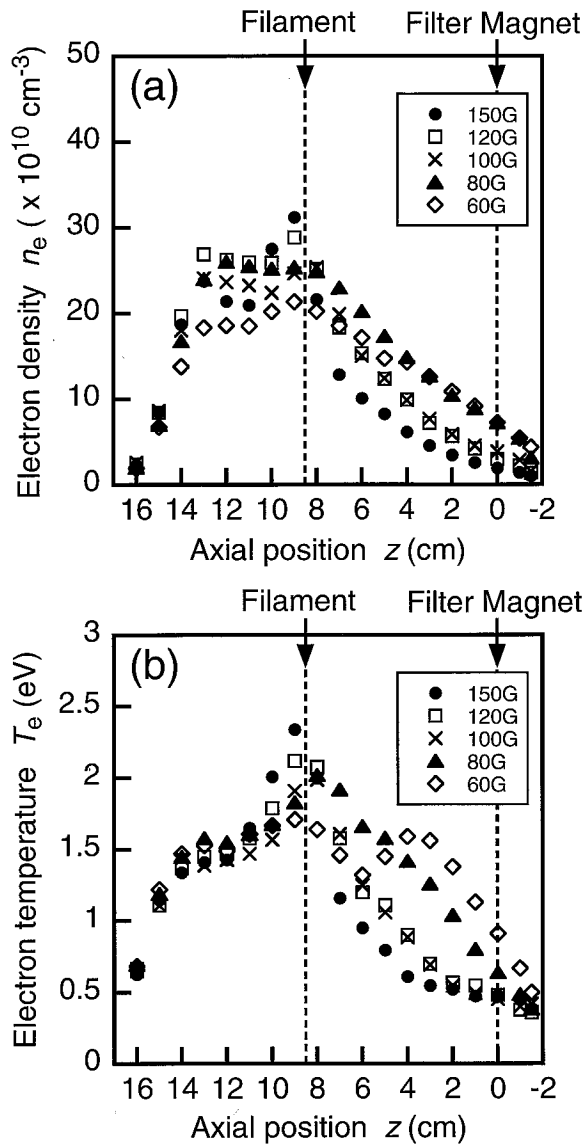


Figure 2. Axial distributions of plasma parameters (a) n_e and (b) T_e in H_2 plasmas. Experimental conditions are as follows: discharge voltage $V_d = 70$ V, discharge current $I_d = 5$ A, gas pressure $p(H_2) = 0.2$ Pa. Parameter is the peak magnetic field intensity of the magnetic filter (MF).

should be reduced below 1 eV while keeping n_e high. To realize this condition, namely to enhance H^-/D^- production by dissociative attachment and to reduce H^-/D^- destruction by electron detachment due to collisions with energetic electrons, the MF is used. For this purpose, plasma parameter control is studied by varying the intensity of the MF.

Figures 2 and 3 show axial distributions of plasma parameters (n_e and T_e) in H_2 and D_2 plasmas, respectively. By varying the intensity of the MF, axial distributions of n_e and T_e in both H_2 and D_2 plasmas are changed strongly in the downstream region (i.e. the region from $z = 8$ to -2 cm) [12–14]. Production and control of D_2 plasmas are almost the same as that of H_2 plasmas.

Figures 2 and 3 show that the main effect of increasing the MF is to decrease both n_e and T_e in the extraction region, i.e. the region from $z = 3$ to -2 cm. Figure 4 shows the numerical results of trajectories for fast primary electrons corresponding to the same magnetic field configuration in the source shown

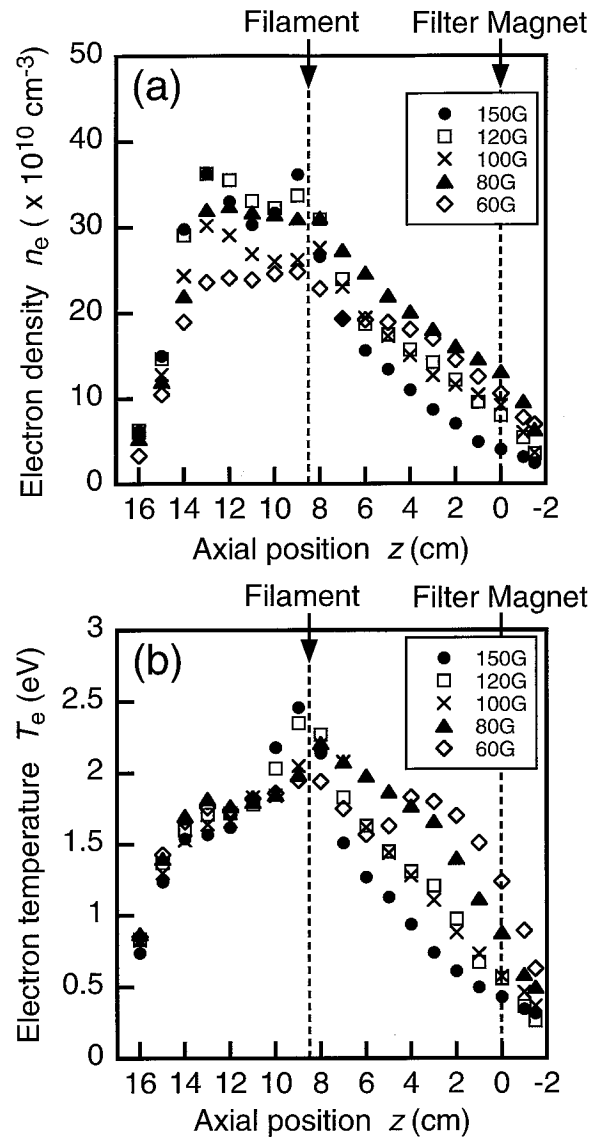


Figure 3. Axial distributions of plasma parameters (a) n_e and (b) T_e in D_2 plasmas. Experimental conditions are as follows: $V_d = 70$ V, $I_d = 5$ A, $p(D_2) = 0.2$ Pa. Parameter is the peak magnetic field intensity of the MF.

in figure 1. It can be seen that decreasing the intensity of the MF allows the fast electrons to approach the extraction region. Namely, ionization collisions will occur more frequently in the downstream region and also increase n_e as shown in figures 2 and 3. In this source, due to the external MF, the width of the half-maximum of the magnetic field intensity is wider (about 16 cm in this case) than in the case of the rod filter [8]. Varying the intensity of the MF also indicates varying the strength of magnetic field distribution in both the source and extraction regions. Thus, the external MF has the merit of changing the plasma parameters in the extraction region whilst having little effect on n_e or T_e upstream of the MF, in the source region, i.e. from $z = 8$ to 16 cm.

As is shown in figures 2 and 3, the axial profiles of n_e and T_e in hydrogen and deuterium plasmas are similar. For comparison, a typical example for axial distributions of n_e and T_e is shown in figure 5, where $B_{MF} = 80$ G. In general, both n_e and T_e in deuterium plasmas are higher than in hydrogen

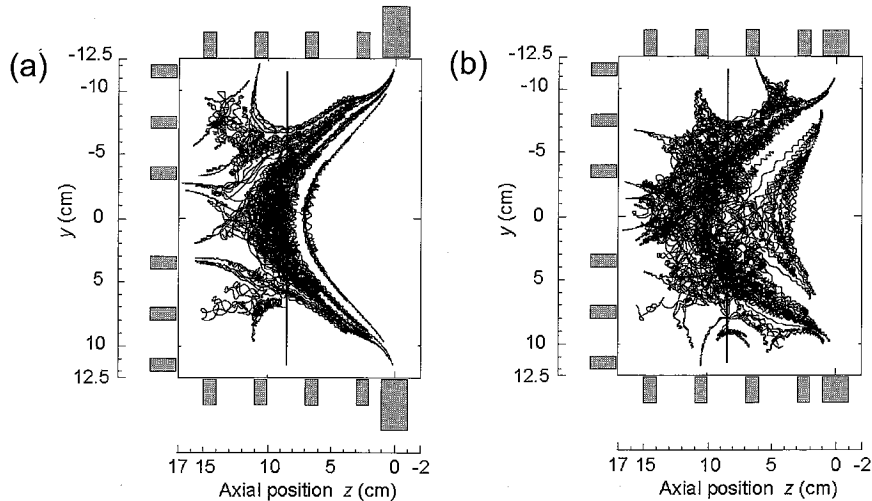


Figure 4. Behaviour of fast primary electrons for two different intensities of the MF: (a) 150 G and (b) 80 G. Trajectories of 20 test particles are plotted. Initial energy of these test particles is set at 80 eV.

plasmas. When $B_{MF} = 60$ G, n_e is slightly higher than that for the case of 80 G. T_e in H_2 plasma is equal to or lower than 1 eV, but T_e in D_2 plasma is above 1 eV in the extraction region. Then, plasma conditions are good for H^- production, but not good for D^- production. When $B_{MF} = 80$ G, values of n_e and T_e in D_2 plasmas are higher than those in H_2 plasmas. T_e in the extraction region is decreased below 1 eV in both H_2 and D_2 plasmas. The plasma conditions are good for H^- and D^- production. A stronger MF field is required to control T_e in D_2 plasmas. This indicates that plasma production and transport are different in H_2 and D_2 plasmas.

Clarifying the dependence of H^-/D^- production on those plasma parameter profiles shown in figures 2 and 3, the variations of H^- and D^- production due to changes in plasma parameter distributions are discussed taking into account main collision processes for production and destruction. Dissociative attachment (DA: $H_2(v'') + e \rightarrow H^- + H$) is the main process for H^- production. For H^- destruction, electron detachment (ED: $H^- + e \rightarrow H + 2e$) and mutual neutralization (MN: $H^+ + H^- \rightarrow H + H$) are dominant. The ED process is very effective for T_e in the range of a few electron volts and the MN process depends slightly on ion temperature. These three processes are also applicable to the main process in D_2 plasmas for D^- production and destruction. As DA and ED processes depends on T_e , in the following discussion, parameter dependence of DA and ED processes is presented, where it is assumed that only $H_2(v'' = 8)$ or $D_2(v'' = 12)$ is present. $H_2(v'' = 8)$ and $D_2(v'' = 12)$ have almost the same internal energy [15]. The values of rate coefficient, $\langle\sigma v\rangle_{DA}$ for DA and $\langle\sigma v\rangle_{ED}$ for ED, and collision frequency, $n_e\langle\sigma v\rangle_{DA}$ and $n_e\langle\sigma v\rangle_{ED}$, are estimated using the measured values of T_e and n_e shown in figures 2 and 3.

Figures 6 and 7 show axial distributions of rate coefficients and collision frequencies of DA and ED processes, in H_2 plasmas and D_2 plasmas, respectively [13, 14]. By varying T_e distributions, as shown in figures 6(a) and 7(a), distributions of ED processes are affected strongly while DA processes remain nearly constant. It is found that the T_e control by varying the intensity of the MF reduces the ED process remarkably. As shown in figures 6(b) and 7(b), taking into account both the T_e and n_e changes, the difference between DA with 150 G and the

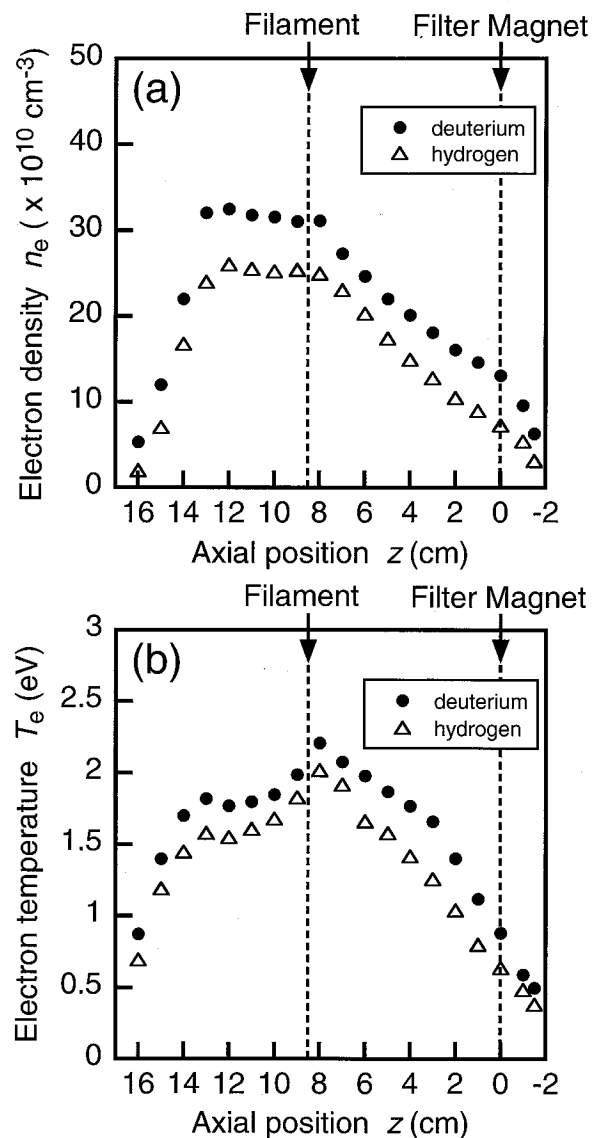


Figure 5. Axial distributions of plasma parameters (a) n_e and (b) T_e in H_2 and D_2 plasmas. Experimental conditions are as follows: $V_d = 70$ V, $I_d = 5$ A, $p(H_2) = p(D_2) = 0.2$ Pa.

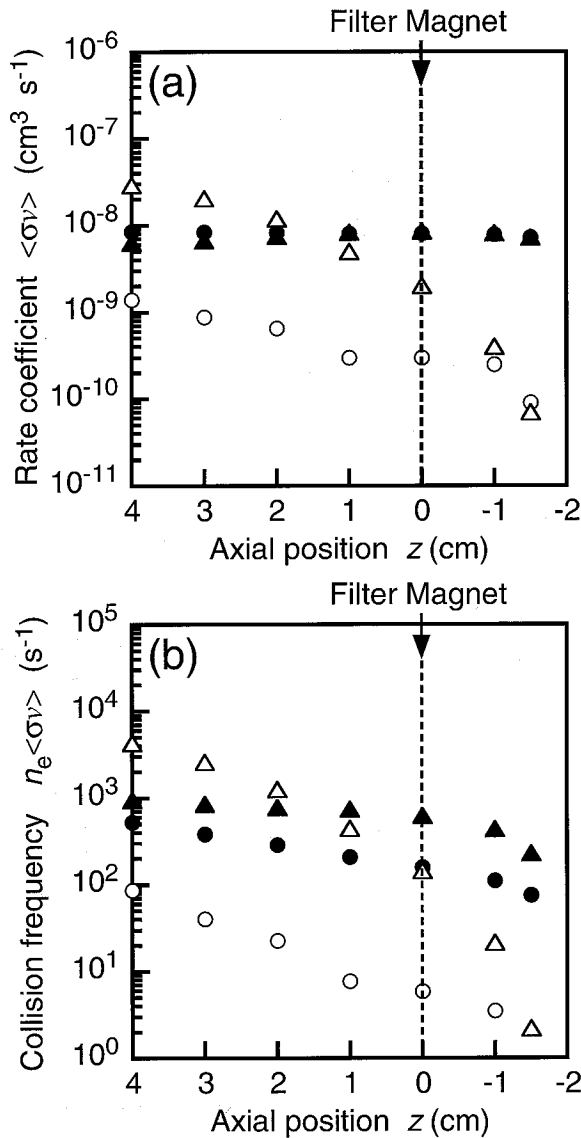


Figure 6. Axial distributions of (a) rate coefficient and (b) collision frequency estimated by measured T_e and n_e in H_2 plasmas (closed circle; H^- production with 150 G, closed triangle; H^- production with 80 G, open circle; H^- destruction with 150 G, open triangle; H^- destruction with 80 G). Corresponding plasma parameters are shown in figure 2.

one with 80 G is caused by the difference between n_e in this region (n_e with 80 G is higher than the one with 150 G).

In the above discussion and in section 3.2, the effects of atoms are not included although they play important roles in destruction processes. As described above, for the destruction of negative ions particularly in the low-pressure case, two processes (i.e. the ED process and MN process) are dominant. The ED process can be minimized by reducing T_e to approximately 1–1.5 eV, but then the MN process will take over. Also, now we do not have sufficient information to estimate atomic density. In some experiments [3, 5], it is reported that the atomic density is higher in D_2 plasmas than in H_2 plasmas. If atoms play an important role in the destruction processes then this could lead D^- densities to be lower than H^- densities in otherwise similar plasmas.

Measured line radiation gives, to a first approximation, information about the population of an electronically excited

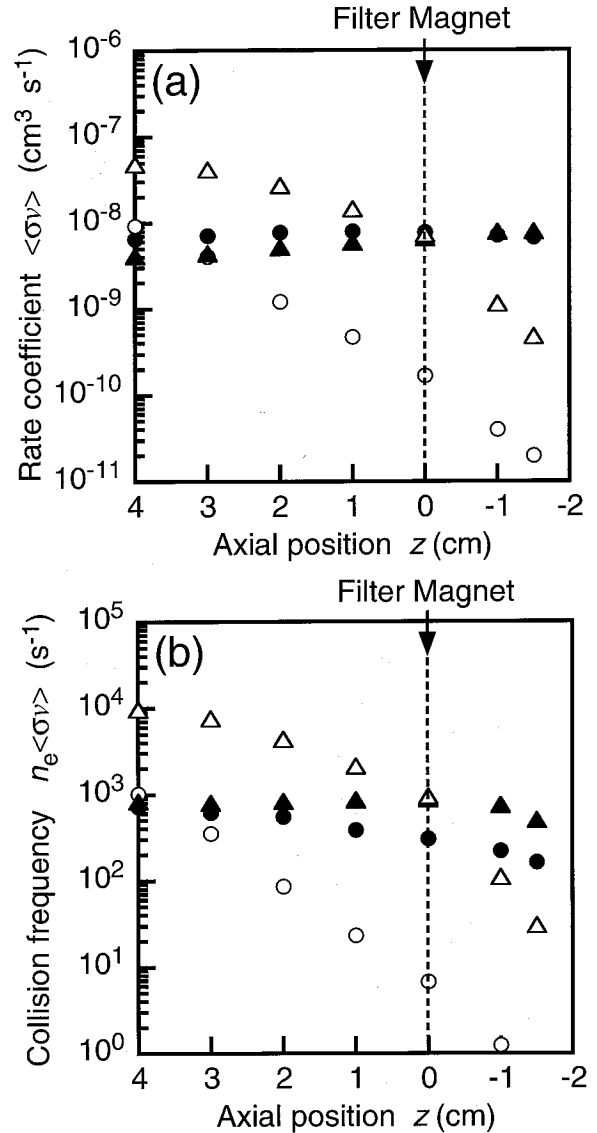


Figure 7. Axial distributions of (a) rate coefficient and (b) collision frequency estimated by measured T_e and n_e in D_2 plasmas (closed circle; D^- production with 150 G, closed triangle; D^- production with 80 G, open circle; D^- destruction with 150 G, open triangle; D^- destruction with 80 G). Corresponding plasma parameters are shown in figure 3.

state. The relation with the ground state population, and thus with the particle density, is obtained from the population models, the so-called collisional radiative models. In the present experiment, Lyman- α intensity is lower in the D_2 plasma than in the H_2 plasma. We now prepare the experiments on the effects of Cs injection. The atomic density at the PG determines the efficiency of formation of negative ions by the surface effect whereas the molecular density is the basis for formation by the volume mechanism. In the future experiment, we will further discuss the isotope effect of H^- and D^- production including the effect of the atomic density.

3.2. Production and extraction of negative ions

As shown in figures 2 and 2, the plasma parameters in the extraction region depend strongly on the MF intensity, and therefore plasma conditions for negative ion volume

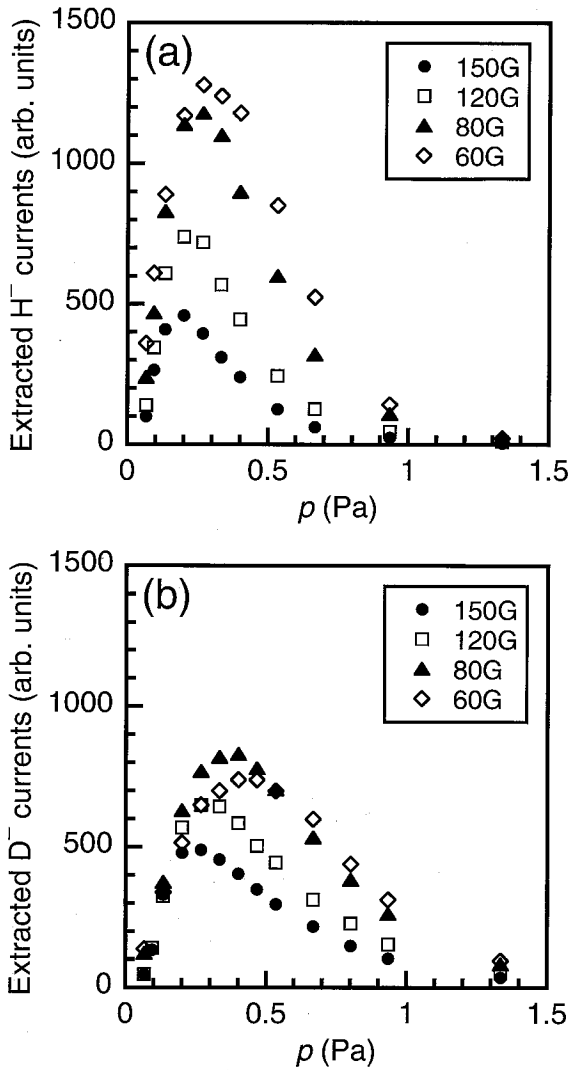


Figure 8. Pressure dependences of extracted (a) H^- and (b) D^- currents. Experimental conditions are as follows: $V_d = 70$ V, $I_d = 5$ A and extraction voltage $V_{ex} = 1.5$ kV. The parameter is the magnetic field intensity of the MF.

production are also varied. As a consequence the extracted negative ion currents are found to be strongly dependent on the MF intensity.

Figure 8 shows the pressure dependence of the extracted negative ion currents from (a) H_2 and (b) D_2 plasmas [12]. In both cases, as described above, the negative ion currents are varied due to the change in plasma conditions by decreasing the MF intensity. In both cases, there are also some optimum pressures. With increasing gas pressure, negative ion currents (i.e. the H^- current, I_{H^-} and the D^- current, I_{D^-}) increase in their magnitude, reach the maximum value and then decrease. Decreasing MF intensity, the optimum pressure p_{opt} shifts to higher pressure. For D^- production, p_{opt} is from 0.27 to 0.47 Pa. On the other hand, for H^- production, p_{opt} is from 0.2 to 0.27 Pa. Optimum pressure in D_2 plasmas is slightly higher than in H_2 plasmas.

H^- density distributions across the MF have been measured using the photodetachment technique and the dependence of the H^- density on plasma parameters have been studied. Figure 9 shows axial distributions of H^- ion densities, where $B_{MF} = 150$ G and 80 G, respectively [13, 14].

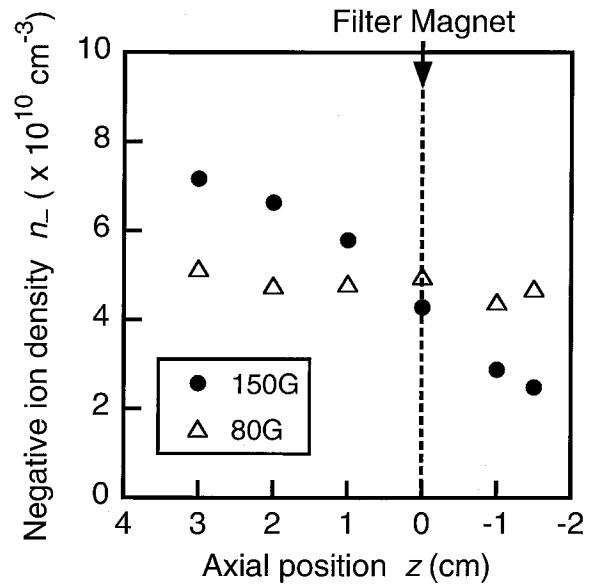


Figure 9. Axial distributions of H^- ion densities. Experimental conditions are as follows: $V_d = 70$ V, $I_d = 5$ A and $p(H_2) = 0.2$ Pa. The parameter is the magnetic field intensity of the MF. Corresponding plasma parameters are shown in figure 2 (with $B_{MF} = 150$ G and 80 G).

Plasma parameters corresponding to these H^- ion densities are shown in figure 2. Spatial distributions of H^- densities vary if plasma parameters change. When $B_{MF} = 150$ G, the H^- density distribution decreases towards the extraction hole (i.e. $z = -2.5$ cm). On the other hand, when $B_{MF} = 80$ G, the H^- density distribution remains a nearly constant value even though n_e decreases towards the extraction hole. In front of the extraction hole (i.e. plots at $z = -1.5$ cm), the H^- density with 80 G is higher than that with 150 G by a factor about 2. As is shown in figure 8, extracted H^- currents from the source are also in the same ratio, showing that the extracted H^- currents are, to a first approximation, proportional to the H^- densities in front of the extraction hole.

D^- density distributions are compared with H^- density distributions in the same discharge condition. Figure 10 shows axial distributions of negative ion densities, where $B_{MF} = 80$ G, $p(H_2) = p(D_2) = 0.2$ Pa, respectively [13, 14]. Axial distribution of D^- density is lower than that of H^- density. Figures 2 and 3 show that T_e in D_2 plasmas is higher than that in H_2 plasmas. As discussed in section 3.1 (see figure 7), the effect of the destruction of D^- by the ED process on the D^- density is higher than the effect on the H^- density in a similar H_2 plasma. As shown in figure 8, the extracted D^- current is also lower than the H^- current, and the ratio of H^- to D^- current is almost the same as the ratio of H^- to D^- density in front of the extraction hole. Therefore, the extracted D^- current is mainly determined by the D^- density in front of the extraction hole. Detailed discussions in relation to negative ion densities in the source and extracted negative ion currents are given below.

Using measured values of the negative ion temperature, the relationship between negative ion densities in the source and the extracted negative ion currents was studied by Leroy *et al* [16]. We also study this relation. Figure 11 shows axial distributions of negative ion densities in the source, where the field intensity of the MF is 80 G, $p(H_2) = 0.2$ Pa

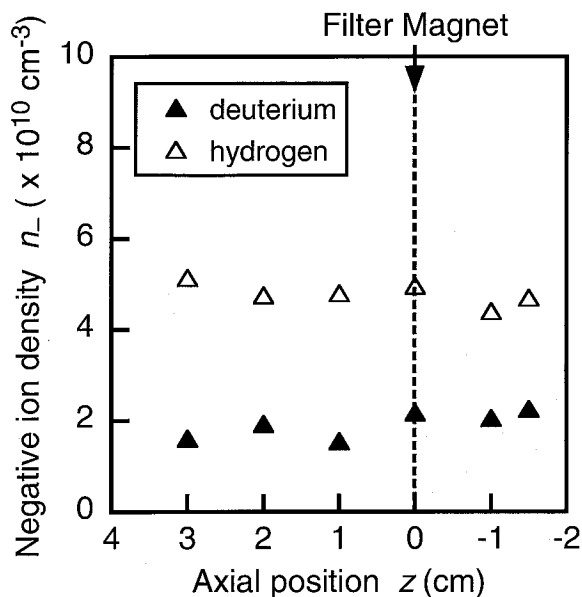


Figure 10. Axial distributions of H^- and D^- ion densities. Experimental conditions are as follows: $V_d = 70$ V, $I_d = 5$ A, $p(H_2$ or $D_2) = 0.2$ Pa and $B_{MF} = 80$ G. Corresponding plasma parameters are shown in figures 2 (for H_2 plasma) and 3 (for D_2 plasma).

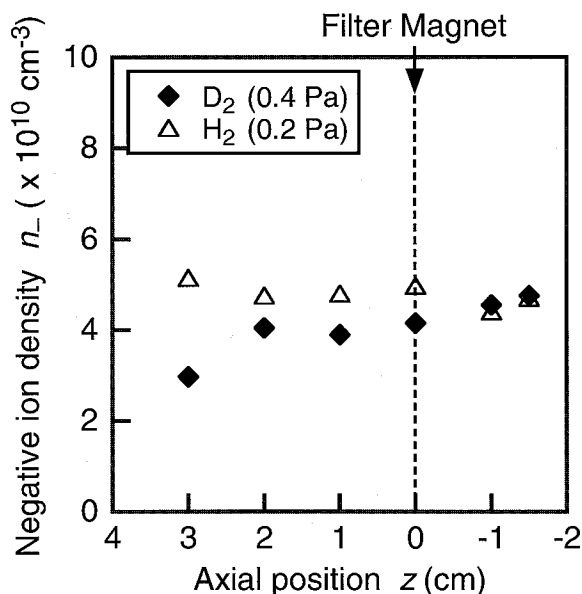


Figure 11. Axial distributions of H^- and D^- ion densities. Experimental conditions are as follows: $V_d = 70$ V, $I_d = 5$ A, $p(H_2) = 0.2$ Pa, $p(D_2) = 0.4$ Pa and $B_{MF} = 80$ G.

and $p(D_2) = 0.4$ Pa, respectively [11]. These two different pressure conditions correspond to the results in figure 8. As shown in figure 11, the negative ion densities in front of the extraction hole in D_2 plasmas are nearly equal to those in H_2 plasmas. On the other hand, according to the results in figure 8, I_{D^-} at 0.4 Pa with 80 G is lower than I_{H^-} at 0.2 Pa, when the same extraction voltage V_{ex} is applied. The ratio of the two currents is approximately $\sqrt{2}$. If the D^- and H^- have the same temperature and if the extracted currents are proportional to the thermal ion flux to the extraction hole then the factor of $\sqrt{2}$ can be simply explained by the mass difference. If that is the case, the D^- ion densities in the source at 0.4 Pa are the same as the

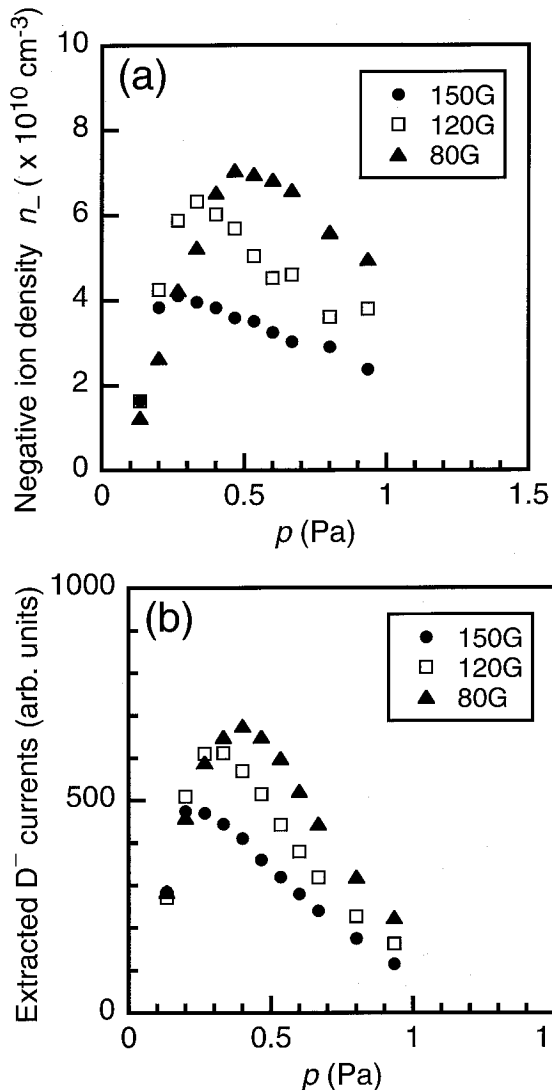


Figure 12. Pressure dependences of (a) D^- ion densities in the source and (b) the extracted D^- currents. Experimental conditions are as follows: $V_d = 70$ V, $I_d = 5$ A and $V_{ex} = 1.5$ kV. D^- ion densities are measured at $z = -0.5$ cm. Extraction hole is set at $z = -1.5$ cm. Parameter is the magnetic field intensity of the MF.

H^- ion densities in the source at 0.2 Pa. The results shown in figure 11 support this.

Figure 12 shows pressure dependence of (a) the D^- ion densities in the source and (b) the extracted D^- currents, where the intensity of the MF is a parameter. In the high pressure range from 0.4 to 0.93 Pa, taking into account the variation in the negative ion density, the change in the accelerated current indicates the presence of the stripping loss of the latter. As a whole, the patterns of pressure dependence in the D^- ion densities are nearly the same as those in the extracted D^- currents. Namely, the extracted D^- currents are proportional to the D^- densities in the source. According to the results shown in figures 9–12, the values of the extracted negative ion currents are mainly determined by the negative ion densities in front of the extraction hole.

3.3. VUV emission measurement

As discussed above, plasma parameters, H^- densities and extracted H^- currents are changed by varying the intensity

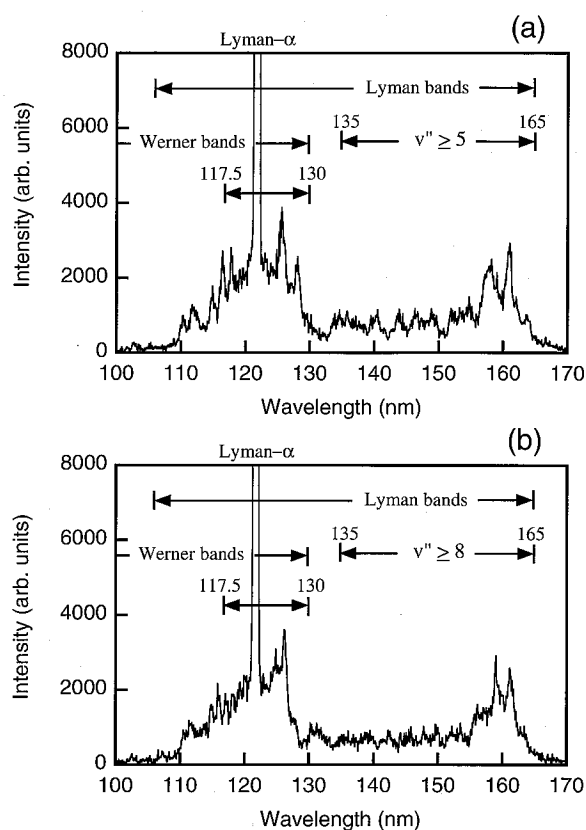


Figure 13. Typical VUV spectra from (a) H_2 and (b) D_2 plasmas. Experimental conditions are as follows: $V_d = 70$ V, $I_d = 5$ A, $p(\text{H}_2) = p(\text{D}_2) = 0.4$ Pa and $B_{\text{MF}} = 80$ G.

of the MF. Here, we discuss the relationship between H^- production and $\text{H}_2(v'')$ production with the measurement of the VUV emission. VUV emission measurement has been done in a preliminary way. The VUV spectra were detected at $z = 8.5$ cm in the source region.

Figure 13 shows the typical VUV spectra from both (a) H_2 and (b) D_2 plasmas. The signal at 121.6 nm in H_2 plasmas is from Lyman α . Because H and D are isotopes, we expect that the spectrum from the Lyman bands from D_2 plasmas is similar to that from the H_2 plasmas. As shown in figure 13, the spectra are similar, but not identical. According to the numerical results [2], $\text{H}_2(v'' \geq 5)$ are more effective for H^- production. In figure 13(a), spectra leading to the production of $\text{H}_2(v'' \geq 5)$ ranged from 117.5 to 165 nm [7]. Internal energy of deuterium molecules $\text{D}_2(v'' \geq 8)$ is the same as that of $\text{H}_2(v'' \geq 5)$. Therefore, the discussion on VUV spectra in H_2 plasmas should also be applicable to the discussion on VUV spectra in D_2 plasmas. Namely, the production of highly vibrationally excited deuterium molecules $\text{D}_2(v'')$ is related to the emission with the same wavelength range, i.e. 117.5 ~ 165 nm. We obtain the total intensity of the VUV spectra by integrating from 110 to 170 nm in both H_2 and D_2 plasmas. In the integration of VUV spectra, Lyman α is excluded because it is not concerned with the production of vibrationally excited molecules. In the following paragraphs, these integrated intensities are presented for discussing production of $\text{H}_2(v'')$ and $\text{D}_2(v'')$.

Figure 14 shows the pressure dependence of the integrated intensities of VUV spectra from H_2 plasmas, where the intensity of the MF is a parameter. Plasma parameters, H^- densities and extracted H^- currents corresponding to these

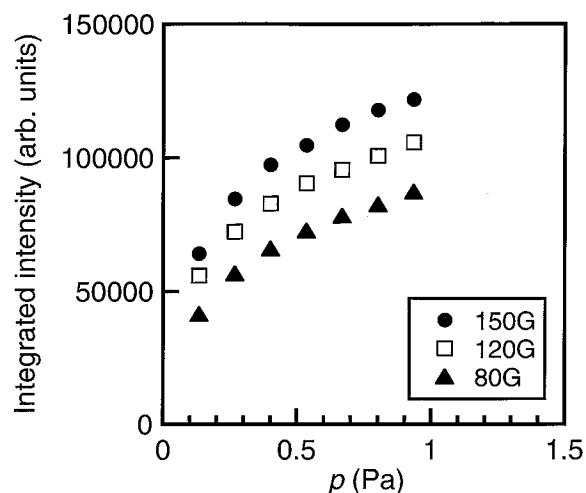


Figure 14. Pressure dependence of the integrated intensities of VUV spectra from H_2 plasmas. Experimental conditions are as follows: $V_d = 70$ V, $I_d = 5$ A. The parameter is the magnetic field intensity of the MF.

VUV emissions are shown in figures 2, 8(a) and 9, respectively. The VUV emissions increased gradually with gas pressure. The values of integrated intensities with 150 G are highest in the entire region of gas pressure, and the intensities are decreased with the intensity of the MF. As shown in figure 8(a), the extracted H^- currents vary with the intensity of the MF and, for a fixed value of the MF, there is an optimum pressure (i.e. 0.2–0.27 Pa), which increases with decreasing intensity of the MF. It is noted that the integrated intensity of the VUV emissions and the extracted H^- currents vary in opposite directions, respectively, when the MF is varied. Figure 4 shows that the trajectories of primary fast electrons, in the case of $B_{\text{MF}} = 150$ G, are concentrated around the filaments and that the density of fast electrons in the extraction regions is higher for $B_{\text{MF}} = 80$ G. Numerical calculations [17] show that the VUV emissions associated with the process (1b) are a function of the fast electron density. Therefore, as the VUV measurements were made in the source region, these should be higher with $B_{\text{MF}} = 150$ G than with $B_{\text{MF}} = 80$ G. We have also confirmed the same tendencies on the discharge power dependences between VUV emissions and H^- currents as those on pressure dependences of the above-mentioned MF intensities.

According to the results shown in figures 2, 8 and 14 and related discussions, our present picture on negative ion production is as follows: in the present experimental conditions with low pressure, electron–neutral collision mean free paths for destruction of the vibrationally excited hydrogen molecules $\text{H}_2(v'')$ (i.e. ionization and dissociation collisions) are a few tens of centimetres. Therefore, sufficient amount of $\text{H}_2(v'')$ are transported to the extraction region, although $\text{H}_2(v'')$ are produced by the collisions between the ground state hydrogen molecules H_2 and the fast primary electrons in the source region. The negative ions are produced by the DA process of slow plasma electrons to $\text{H}_2(v'')$ in the extraction region. Namely, negative ion production is rate-determined by the plasma parameters in the extraction region.

VUV emissions from D_2 plasmas are measured in order to be able to assess the production of $\text{D}_2(v'')$. Figure 15

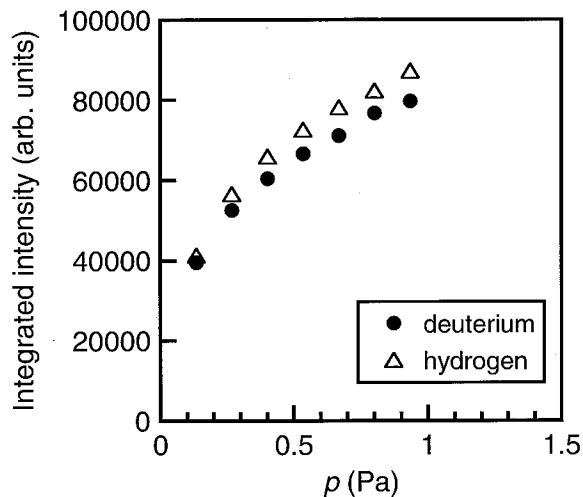


Figure 15. Pressure dependence of the integrated intensities of VUV spectra from H_2 and D_2 plasmas. Experimental conditions are as follows: $V_d = 70$ V, $I_d = 5$ A and $B_{MF} = 80$ G.

shows the pressure dependence of the integrated intensities of VUV spectra from H_2 and D_2 plasmas, where $B_{MF} = 80$ G. While the difference in the integrated intensities between H_2 and D_2 plasmas increase slightly with gas pressure, the ratio of the VUV emission from D_2 to that from H_2 plasmas is about 0.9–0.95. VUV emission intensities from D_2 plasmas are nearly equal to or slightly lower than that from H_2 plasmas. On the other hand, theoretical results show that the ratio of excitation collision cross section of $D_2(v'')$ to that of $H_2(v'')$ [18] is about 0.7. As the excitation collision cross section is not estimated directly from the experimental results of the integrated emission intensities shown here, then these experimental results cannot be compared with theory. Nevertheless, the present experimental results of VUV emission may suggest that the density of the produced $D_2(v'')$ is rather high compared with the expected density of $D_2(v'')$.

According to the results of the H^- and D^- ions extraction shown in figure 8, the characteristics of the extracted H^- and D^- currents are different from each other. The values of the extracted H^- currents are increased markedly by decreasing the field intensity of the MF. Namely, the value of I_{H^-} is varied from the maximum value of 460 (for $B_{MF} = 150$ G) to that of 1280 (for $B_{MF} = 60$ G) by a factor about 2.8. Although the extracted D^- currents also increase by decreasing the field intensity of the MF, the value of I_{D^-} is varied from a maximum value of 480 (for $B_{MF} = 150$ G) to that of 830 (for $B_{MF} = 80$ G) by a factor about 1.7. Then, the amplification factor of I_{D^-} is lower than that of I_{H^-} under the same discharge conditions. Taking into account the above discussion on the VUV emissions and transport of the vibrationally excited molecules, it is now not concluded that the difference in the extracted negative ion currents is caused by the difference in the vibrationally excited molecules.

In the future, VUV emissions from H_2 and D_2 plasmas will be further studied to discuss the difference in the characteristic features of the extracted H^- and D^- currents. We have previously calculated that the extraction probability of negative ions depends strongly on the upstream distance from the extraction grid [19,20]. To increase the extraction of

negative ion currents, the production of negative ions near the extraction grid should be enhanced by optimizing the plasma conditions.

4. Summary

Production and control of H_2 and D_2 plasmas are performed by varying the intensity of the MF. The values of T_e and n_e in D_2 plasmas are slightly higher than those in H_2 plasmas. T_e in D_2 plasmas cannot be decreased and is kept above 1 eV in the extraction region with the same MF intensity for optimizing H_2 plasmas. A stronger MF field is required for the control of T_e in D_2 plasmas. Therefore, plasma production and/or transport in H_2 is different from that in D_2 , i.e. an isotope dependence of plasma production is observed. H^- and D^- densities have different spatial distributions corresponding to different plasma parameters. The extracted H^- and D^- currents are mainly determined by H^- and D^- densities in front of the extraction hole, respectively. According to the discussions based on the estimated rate coefficients and the collision frequencies of main collision processes for production and destruction of negative ions, it is reconfirmed that T_e in the extraction region should be reduced below 1 eV while keeping n_e higher for the enhancement of H^- and D^- production. For further studying the enhancement of D^- production, preliminary results of simultaneous measurements of VUV emission and negative ion density in the source are presented and an isotope effect of H^-/D^- volume production is briefly discussed. In the future, we will discuss further the isotope effect of H^- and D^- production including Cs injection and the atomic density.

Acknowledgments

The authors would like to thank Professor Y. Takeiri and Dr K. Tsumori (National Institute for Fusion Science) for their valuable discussions. The authors also thank Professors H. Naitou and Y. Tauchi (Yamaguchi University) for their discussion and support in the experiments. A part of this work was supported by the Grant-in-Aid for Scientific Research from the Ministry of Education, Culture, Sports, Science and Technology, Japan. This work was also performed with the support of the NIFS LHD Project Research Collaboration.

References

- [1] Hiskes J.R. and Karo A.M. 1984 *J. Appl. Phys.* **56** 1927
- [2] Fukumasa O. 1989 *J. Phys. D: Appl. Phys.* **22** 1668
- [3] Pealat M., Taran J-P.E., Bacal M. and Hillion F. 1985 *J. Chem. Phys.* **82** 4943
- [4] Inoue T., Ackerman G.D., Cooper W.S., Hanada M., Kwan J.W., Ohra Y., Okumura Y. and Seki M. 1990 *Rev. Sci. Instrum.* **61** 496
- [5] Fantz U., et al IAEA-Technical Meeting on Negative Ion Based Neutral Beam Injection (Padova, May 2005) p 7
- [6] Fukumasa O., Tauchi Y., Yabuki Y., Mori S. and Takeiri Y. 2002 *Proc. 9th Int. Symp. on the Production and Neutralization of Negative Ions and Beams (Gif-sur-Yvette, France) (AIP Conf. Proc. 639)* p 28
- [7] Graham W.G. 1984 *J. Phys. D* **17** 2225

- [8] Fukumasa O., Mizuki N. and Niitani E. 1998 *Rev. Sci. Instrum.* **69** 995
- [9] Mori S., Tauchi Y., Fukumasa O., Hamabe M. and Takeiri Y. 2003 *Abstracts 30th IEEE Int. Conf. on Plasma Science (Jeju, Korea)* p 209
- [10] Fukumasa O. 2003 *Proc. 26th Int. Conf. on Phenomena in Ionized Gases (Greifswald, Germany)* vol 1 p 13
- [11] Bacal M. and Hamilton G.W. 1979 *Phys. Rev. Lett.* **42** 1538
- [12] Fukumasa O., Mori S., Nakada N., Tauchi Y., Hamabe M., Tsumori K. and Takeiri Y. 2004 *Contrib. Plasma Phys.* **44** 516
- [13] Mori S., Tauchi Y., Fukumasa O., Hamabe M., Tsumori K. and Takeiri Y. 2005 *Novel Materials Processing by Advanced Electromagnetic Energy Sources (MAPEES'04)* ed S. Miyake (Oxford: Elsevier) pp 55–8
- [14] Mori S. and Fukumasa O. 2006 *Thin Solid Films* **506–507** 531
- [15] Wadehra J.M. 1979 *Appl. Phys. Lett.* **35** 917
- [16] Leroy R., Bacal M., Berlemont P., Courteille C. and Stern R.A. 1992 *Rev. Sci. Instrum.* **63** 2686
- [17] Mori S. and Fukumasa O. *IEE Japan.* (in Japanese) submitted
- [18] Celiberto R., Capitelli M. and Lamanna U.T. 1994 *Chem. Phys.* **183** 101
- [19] Fukumasa O. and Nishida R. 2004 *Proc. 10th Int. Symp. on the Production and Neutralization of Negative Ions and Beams (Kiev, Ukraine) (AIP Conf. Proc. 763)* p 159
- [20] Fukumasa O. and Nishida R. 2006 *Nucl. Fusion* **46** at press